Experimental results and theoretical model to describe angular dependence of light scattering by monolayer of nematic droplets

V.A. Loiko[a,*], M.N. Krakhalev[b,c], A.V. Konkolovich[a], O.O. Prishchepa[b,c], A.A. Miskevich[a], V.Ya. Zyryanov[b]

[a] *Stepanov Institute of Physics of the National Academy of Sciences of Belarus, Minsk 220072, Belarus*
[b] *Kirensky Institute of Physics, Krasnoyarsk Scientific Center, Russian Academy of Sciences, Krasnoyarsk 660036, Russia*
[c] *Siberian Federal University, Krasnoyarsk, 660041, Russia*

[*] E-mail: *loiko@dragon.bas-net.by, tel: +375 (17) 284-2894, fax: +375 (17) 284-0879*

Abstract

Light scattering by a monolayer of bipolar nematic droplets encapsulated in polymer film is examined both experimentally and theoretically. A method for the simulation of the angular distribution of scattered light is based on the anomalous diffraction and interference approximations taking into account the director configuration within liquid crystal droplets and their bipolar axes orientation. The director configuration in nematic droplets is calculated using the relaxation method of the free energy minimization. The characteristics of the sample, including distribution of droplet sizes and shape anisometry, are measured in details. The experimental results and theoretical data agree closely with each other.

Keywords: Polymer-dispersed liquid crystal film, Liquid crystal droplet, Director configuration, Light scattering, Monolayer of droplets.

1. Introduction

The ensemble of optically anisotropic particles is not a trivial object for the evaluation of its light scattering characteristics [1]. This issue becomes even more complicated if to consider liquid crystal (LC) droplets [2-7], for example, polymer-dispersed liquid crystal (PDLC) films because orientation structure within the droplets is commonly inhomogeneous. Configuration of LC director (a unit vector **n** characterizing preferred molecular orientation for a local volume in a droplet) can be rather complicated [2,3,7]. Consecutive development of special simulation techniques by many research groups (see, for instance, the lists of some of them in [6,7]) allows now calculating adequately the light scattering pictures for actual LC dispersions.

In this paper, we perform comparison of the theoretical estimations and experimental data on angular distribution of light scattered by a PDLC film with monolayer of bipolar nematic droplets. This theoretical approach takes into account distributions of droplet in size and shape anisotropy, orientation of droplets, and director configuration in LC droplets. The last is calculated using the relaxation method of the elastic energy minimization [2,3].

2. Materials and sample preparation

The samples have been made based on nematic liquid crystal 4-n-pentyl-4'-cyanobiphenyl (5CB) dispersed in polyvinylbutyral (PVB). Weight ratio of the components was 5CB: PVB = 53 : 47. Solvent induced phase separation (SIPS) method using the ethyl alcohol as a common solvent was applied to prepare the samples. Heterogeneous films of polymer-dispersed liquid crystal were formed on the glass substrate in the result of solvent evaporation during 24 hours at the room temperature.

Refractive indices of 5CB [8] measured at $t = 23$ ˚C and $\lambda = 0.633$ μm are $n_{\|} = 1.717$, $n_{\perp} = 1.531$, where the symbols || and ⊥ show the mutual orientation of the electrical vector of light wave and the LC director. Refractive index of pure PVB is $n_p = 1.490$ at $\lambda = 0.633$ μm. However, during the phase separation the part of LC remains dissolved in matrix [9] matching the refractive indices $n_{\perp 5CB}$ and n_p. To estimate the refractive index of polymer matrix we used the composite with the maximal LC content at which the phase separation has not occurred yet. In our case this requirement was satisfied for the composite at the weight ratio of the components being 5CB : PVB = 26 : 74. The refractive index of such film is $n_{p+LC} = 1.522$ (at $t = 23$ ˚C and $\lambda = 0.633$ μm).

3. Experimental equipment

Scattering intensity was measured by means of the optical set-up shown schematically in Fig. 1. Unpolarized beam of He-Ne laser (LASOS, $\lambda = 0.633$ μm) passed through the polarizer which can turn from the horizontal direction to the vertical one. Linearly-polarized light after polarizer is incident normally on surface of the PDLC sample under study. The intensity of scattering light was measured by the silicon photodetector with the amplifier PDA100A-EC (ThorLabs) arranged on the optical breadboard rotating in the horizontal plane. PDLC film position coincides with the rotation axis of the optical plate. Angular sizes of the optical diaphragm located in front of photodetector are 15 minutes in the horizontal direction and 45 minutes in the vertical one. Intensity of scattered light depending on the angle is measured with the increment 15 ± 2.5 minutes beginning with the 40′ angle relative to the symmetry axis to exclude the forwardly transmitted coherent radiation. The signal from photodetector is analyzed using the oscillograph TDS 2012B (Tektronix).

The turn of polarizer and analyzer relative to each other as well as to the horizontal allows measuring the scattering intensity for the various experimental schemes. We have considered two variants. For the first one the polarizer and analyzer were oriented vertically (*vv*-component of the scattered light). In other case the polarizer orientation was vertical and analyzer one was horizontal (*vh*-component of the scattered light). Transmittance of both polarizer and analyzer for parallel orientation is $T_{\|} = 0.8548$. Their transmittance at the orthogonal orientation is $T_{\perp} = 0.0016$.

Morphology of the composite film was studied by the polarizing optical microscope Axio Imager.A1m (Carl Zeiss) equipped with the digital camera. The obtained digital microphotographs were processed by means of the software AxioVision (Carl Zeiss).

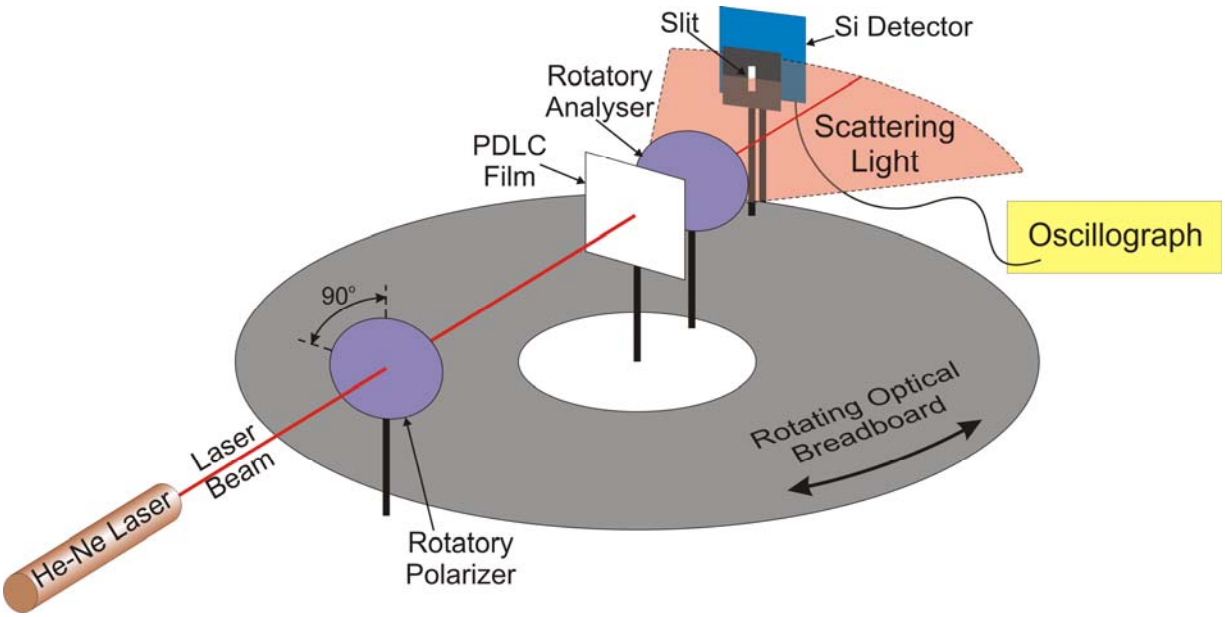

Fig. 1. Scheme of the setup to measure intensity of scattered light.

4. Results of measurements

Prepared PDLC film contains the bipolar nematic droplets with the average diameter 13.5 μm (Fig. 2). The observation of the cross section of the film under study has shown that the average film thickness is 4.3 μm, and ratio of the minor to the major spheroid axes is varied in the range of 0.7 ÷ 0.2 for the droplets with diameters of 6 - 20 μm in the film plane.

Relatively small dispersion of the droplet sizes is observed (Fig. 3). Fraction of droplets in the range of 13.5 ± 2.5 μm is 73 %. The filling factor η of the layer is calculated as the ratio of sum of areas occupied with all droplets within the observable part of the sample to the square of this part. For the film shown in Fig. 2 the filling factor $\eta = 0.23$.

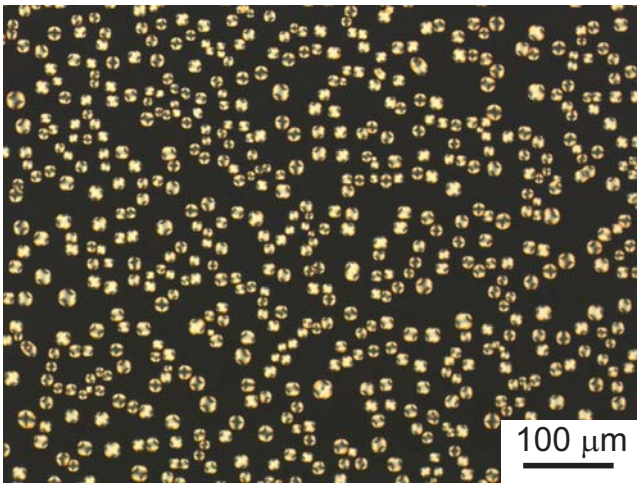

Fig. 2. Microphotograph of the film in the crossed polarizers. The size of the area is 700×520 μm. Polarizers (they are not shown) are oriented along the photo edges.

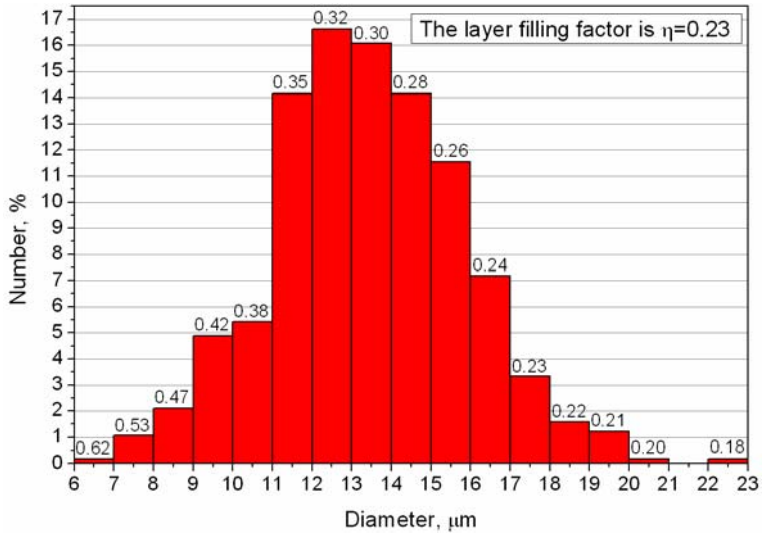

Fig. 3. Distribution of droplet diameters in the film plane. The data over the bars are the values of the ratio of the minor to major droplet axes.

The photographs scattering patterns of the linearly polarized light by the sample under study are shown in Fig. 4. They were obtained by means of the above described set-up. The photodetector and the camera objective were close to the sample. Observations in the schemes of parallel and crossed polarizers show that the part of scattered light has polarization which is perpendicular to the incident light polarization. When the polarization direction of incident light is turned round at the definite angle the scattering pattern entirely turns at the same angle.

The scattering diagrams of the polarized light measured for the parallel and crossed polarizers are presented in Fig. 5. Only 31 % of the incident light passed in the straightforward direction.

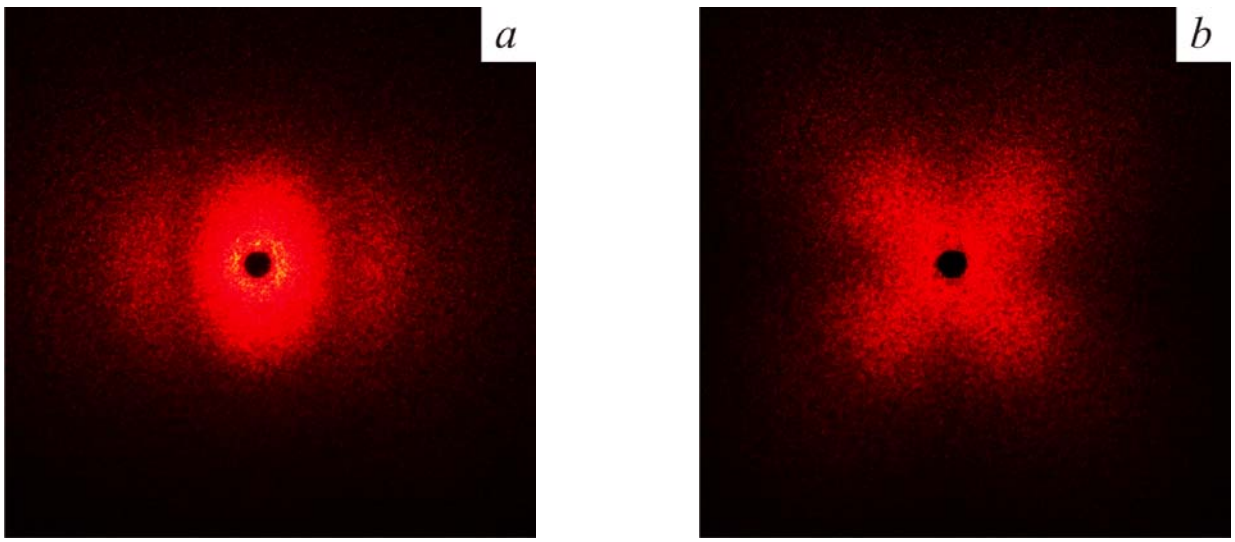

Fig. 4. Photographs of scattering patterns for geometry of parallel (*a*) and crossed (*b*) polarizer and analyzer. The laser beam passing straightforward is shaded. Exposure time for the crossed polarizers is more than for the parallel ones.

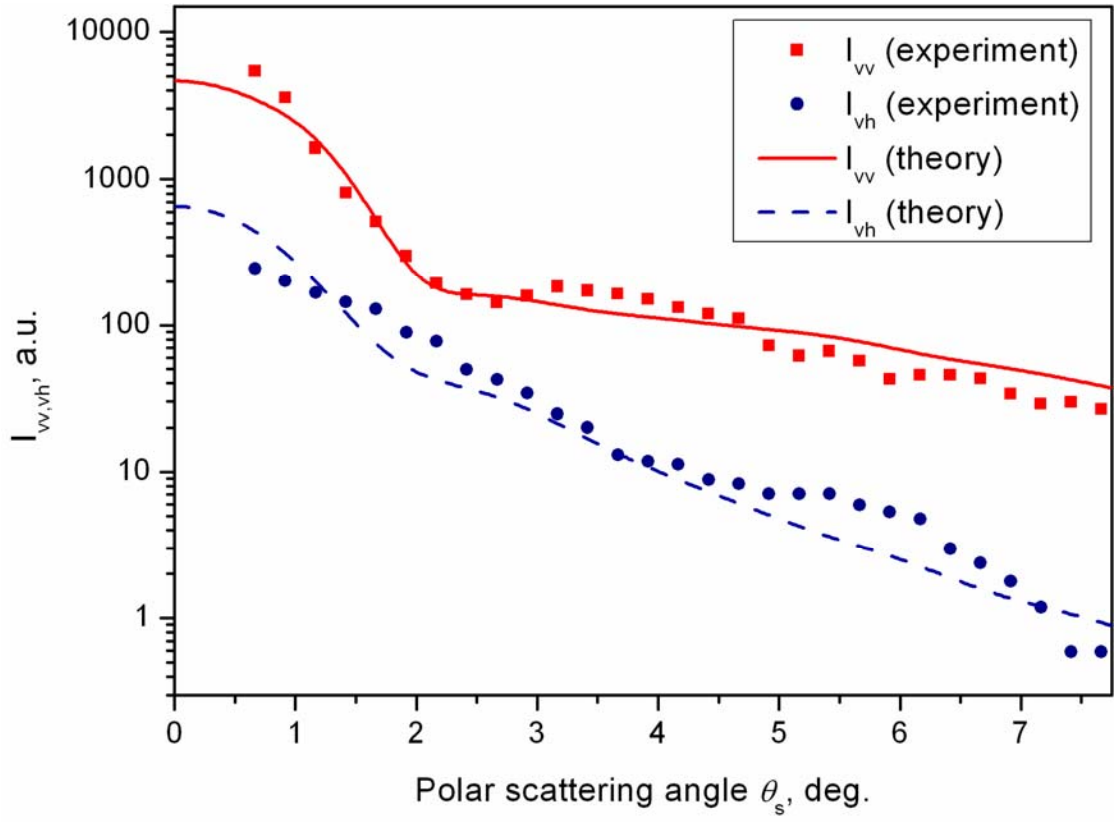

Fig. 5. Experimental and calculated data for the I_{vv} and I_{vh} intensities of light scattered by the PDLC monolayer of spheroidal bipolar LC droplets versus the polar scattering angle θ_s at azimuthal scattering angle φ_s=45°. η=0.23, $n_{||}$ = 1.717, $n_{\perp}$ = 1.531, n_p = 1.522, λ = 0.633 μm.

5. Basic relations to calculate small-angle distribution of light scattered by a PDLC monolayer

Consider a monolayer of PDLC droplets (PDLC monolayer) illuminated by a linearly polarized plane wave with the polarization vector $\mathbf{E}_i$ and wave vector $\mathbf{k}_i$ (Fig.6). In Fg.6 the (*xyz*) denotes the laboratory frame, the *x* axis specifies the direction of propagation of the incident wave, the (*yz*) plane coincides with the monolayer plane, *A* is the part of the layer under consideration, $\mathbf{k}_s$ is the wave vector of scattered wave, θ_s and φ_s are the polar and azimuthal scattering angles, respectively. Unit vector $\mathbf{d}_j$ (droplet director) specifies orientation of the symmetry bipolar axis of the droplet. The *vv* and *vh* lines determine the directions of parallel and orthogonal components of polarization vector of the scattered wave with respect to polarization plane of the incident wave, respectively. The *vv*- and *vh*-components correspond to the geometries of parallel and crossed polarizer and analyzer, respectively.

Let us suppose that PDLC monolayer consists of polydisperse spherical or spheroidal LC droplets with the minor axes normally oriented to the monolayer plane (along the *x* axis of the laboratory frame). To consider the angular distribution of light scattered by the monolayer, we use the interference approximation [12,13].

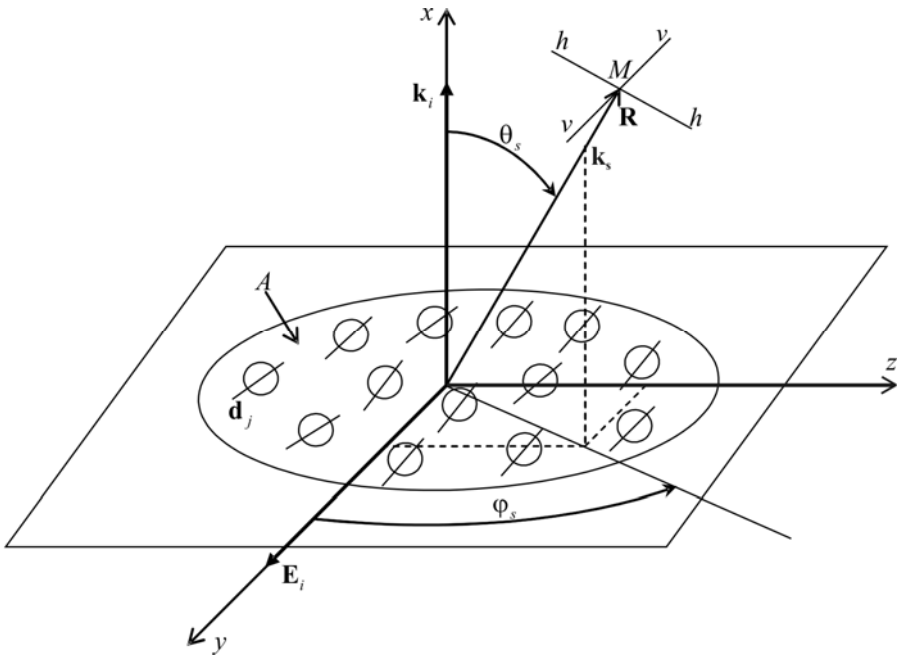

Fig. 6. Schematic presentation of the PDLC monolayer. (*xyz*) is the laboratory frame, (*yz*) is the monolayer plane, $\mathbf{E}_i$ and $\mathbf{k}_i$ are the polarization vector and wavevector of the incident wave, respectively, $\mathbf{k}_s$ is the wavevector of scattered wave, *vv* and *vh* lines determine the directions of parallel and perpendicular components of polarization vector of scattered wave relative to polarization plane of incident wave, $\mathbf{d}_j$ is the director of individual LC droplet. *A* indicates the considered area of the monolayer, **R** is the radius-vector of observation point *M*.

For the far-field observation point determined by the radius-vector **R**, for the *vv*- and *vh*-components of the intensity of incoherently (diffusely) scattered light, it is possible to write:

$$I_{vv}(\theta_s,\varphi_s) = C\frac{\eta}{\langle\sigma\rangle k^2}\left\{\left\langle\left|f_{vv}(\theta_s,\varphi_s)\right|^2\right\rangle + \left|\left\langle f_{vv}(\theta_s,\varphi_s)\right\rangle\right|^2 (S_m(\theta_s)-1)\right\}, \quad (1)$$

$$I_{vh}(\theta_s,\varphi_s) = C\frac{\eta}{\langle\sigma\rangle k^2}\left\{\left\langle\left|f_{vh}(\theta_s,\varphi_s)\right|^2\right\rangle + \left|\left\langle f_{vh}(\theta_s,\varphi_s)\right\rangle\right|^2 (S_m(\theta_s)-1)\right\}. \quad (2)$$

Here $C = AE_i^2/R^2$ is the normalization factor, $\langle\sigma\rangle$ is the average cross section of droplets by the monolayer plane, $\eta = N\langle\sigma\rangle/A$ is the monolayer filling factor (the ratio of the cross section area of LC droplets by the monolayer plane to the area where they are distributed), $k = 2\pi n_p/\lambda$, n_p is the refractive index of the binding polymer matrix, λ is the wavelength of the incident light, the angle brackets $\langle\cdots\rangle$ denote the averaging over the sizes of LC droplets and the structure and orientation of droplet directors $\mathbf{d}_j$, $f_{vv}(\theta_s,\varphi_s)$ and $f_{vh}(\theta_s,\varphi_s)$ are the *vv*- and *vh*-components of the vector amplitude scattering function.

Function $S_m(\theta_s)$ is the structure factor of the polydisperse monolayer. It is found in the framework of the substitution model [14] by averaging the structure factor $S(\theta_s)$ of monodisperse monolayer over the sizes of LC droplets. We use the approximate analytical expression for $S(\theta_s)$ written in [15] as follows:

$$S(\theta_s)=\left\{1+\frac{4\eta}{1-\eta}\frac{2J_1(2kc\sin\theta_s)}{2kc\sin\theta_s}+\frac{4\eta^2}{(1-\eta)^2}J_0(kc\sin\theta_s)\frac{2J_1(kc\sin\theta_s)}{kc\sin\theta_s}+\right.$$
$$\left.+\left(\frac{\eta^2}{(1-\eta)^2}+\frac{2\eta^3}{(1-\eta)^3}\right)\left[\frac{2J_1(kc\sin\theta_s)}{kc\sin\theta_s}\right]^2\right\}^{-1}, \quad (3)$$

where c is the radius of the cross section of single droplet, J_0 and J_1 are the zero- and first-order cylindrical Bessel functions, respectively.

Components of the amplitude function (see Eqs. (1) and (2)) are defined in the terms of the elements S_j (j=1,2,3,4) of the amplitude scattering matrix [16,17] as follows [18]:

$$f_{vv}(\theta_s,\varphi_s)=S_2(\theta_s,\varphi_s)\cos^2(\varphi_s-\varphi_d)+S_1(\theta_s,\varphi_s)\sin^2(\varphi_s-\varphi_d)$$
$$+\frac{1}{2}(S_3(\theta_s,\varphi_s)+S_4(\theta_s,\varphi_s))\sin 2(\varphi_s-\varphi_d), \quad (4)$$

$$f_{vh}(\theta_s,\varphi_s)=S_3(\theta_s,\varphi_s)\sin^2(\varphi_s-\varphi_d)-S_4(\theta_s,\varphi_s)\cos^2(\varphi_s-\varphi_d)+$$
$$\frac{1}{2}(S_2(\theta_s,\varphi_s)-S_1(\theta_s,\varphi_s))\sin 2(\varphi_s-\varphi_d), \quad (5)$$

where φ_d is the azimuthal angle of the droplet director $\mathbf{d}_j$ orientation relative to y axis.

To determine the S_j elements we use the anomalous diffraction approximation (ADA) [16-21]. In this approximation the far field scattered by a droplet is considered as the result of diffraction on the amplitude-phase screen.

For the amplitude scattering matrix elements in the ADA, we have:

$$S_1(\theta_s,\varphi_s)=\frac{k^2\sigma}{2\pi}\int_\sigma(1-T_1(y,z))\exp(-i(ky\cos\varphi_s+kz\sin\varphi_s)\sin\theta_s)dydz, \quad (6)$$

$$S_2(\theta_s,\varphi_s)=\frac{k^2\sigma}{2\pi}\cos\theta_s\int_\sigma(1-T_2(y,z))\exp(-i(ky\cos\varphi_s+kz\sin\varphi_s)\sin\theta_s)dydz, \quad (7)$$

$$S_3(\theta_s,\varphi_s)=-\frac{k^2\sigma}{2\pi}\cos\theta_s\int_\sigma T_3(y,z)\exp(-i(ky\cos\varphi_s+kz\sin\varphi_s)\sin\theta_s)dydz, \quad (8)$$

$$S_4(\theta_s,\varphi_s)=-\frac{k^2\sigma}{2\pi}\int_\sigma T_4(y,z)\exp(-i(ky\cos\varphi_s+kz\sin\varphi_s)\sin\theta_s)dydz. \quad (9)$$

Here $\sigma=\pi c^2$; $T_j(\xi)$ are the elements of the 2×2 Jones matrix $\underline{\underline{T}}$ of the equivalent amplitude-phase screen (j=1,2,3,4).

The Jones matrix $\underline{\underline{T}}$ depends on the internal structure of the LC droplet [21]:

$$\underline{\underline{T}}(y,z)=\begin{pmatrix}T_2(y,z) & T_3(y,z)\\ T_4(y,z) & T_1(y,z)\end{pmatrix}=\prod_{x=x_{inp}(y,z)}^{x_{out}=(y,z)}R^T(x)PR(x). \quad (10)$$

In Eq. (10) $x_{inp}=-\varepsilon c\sqrt{1-(y^2+y^2)/c^2}$ and $x_{out}=+\varepsilon c\sqrt{1-(y^2+y^2)/c^2}$ are input and output coordinates on the LC droplet surface respectively; ε is the anisometry parameter which is the ratio of

the minor to major axes of droplets (for the spheres $\varepsilon = 1$); P is the matrix of the local phase incursion for the extraordinary and ordinary waves; $R(x)$ and $R^T(x)$ are matrices of the coordinate transformation over the local bases trajectories,

$$P = \begin{pmatrix} \exp\left(ik(n_e(x)/n_p - 1)\Delta x\right) & 0 \\ 0 & \exp\left(ik(n_o/n_p - 1)\Delta x\right) \end{pmatrix}, \tag{11}$$

$$R(x) = \begin{pmatrix} \cos(\varphi(x) - \varphi_s) & -\sin(\varphi(x) - \varphi_s) \\ \sin(\varphi(x) - \varphi_s) & \cos(\varphi(x) - \varphi_s) \end{pmatrix}, \tag{12}$$

$$R^T(x) = \begin{pmatrix} \cos(\varphi(x) - \varphi_s) & \sin(\varphi(x) - \varphi_s) \\ -\sin\varphi(\varphi(x) - \varphi_s) & \cos(\varphi(x) - \varphi_s) \end{pmatrix}, \tag{13}$$

$n_e(x)$ is the local refractive index for extraordinary wave in point $x=x(y,z)$, n_o is the coordinate-independent refractive index for ordinary wave equal to the ordinary refractive index $n_\perp$ of LC, Δx is the longitudinal (along the wavevector of incident wave) size of LC droplet elementary volume in which liquid crystal orientation structure is assumed as uniform and determined by only molecular order parameter [7,22-24], $\varphi(x)$ is the azimuthal angle of local principal plane orientation,

$$n_e(x) = n_\parallel n_\perp / \sqrt{n_\parallel^2 n_x^2 + n_\perp^2 (1 - n_x^2)}\,, \tag{14}$$

$$\cos(\varphi(x) - \varphi_s) = \left(n_y \cos\varphi_s + n_z \sin\varphi_s\right) / \sqrt{1 - n_x^2}\,, \tag{15}$$

$$\sin(\varphi(x) - \varphi_s) = \left(n_z \cos\varphi_s - n_y \sin\varphi_s\right) / \sqrt{1 - n_x^2}\,. \tag{16}$$

In Eqs. (14)-(16), $n_\parallel$ is the extraordinary refractive index of liquid crystal, n_x, n_y, and n_z are the Cartesian components of local director $\mathbf{n}(\mathbf{r})=(n_x, n_y, n_z)$.

Eqs. (1)-(16) allow one to analyze small-angle light scattering by monolayer of polydisperse spherical or spheroidal LC droplets with arbitrary internal structure including the droplets with the inhomogeneous boundary conditions in polymer matrix [25]. Such an analysis requires the determination of internal structure of local director (director configuration) $\mathbf{n}(\mathbf{r})$, the calculation of *vv*- and *vh*-components of vector amplitude scattering function, and the average over the sizes of LC droplets and orientations of their directors.

In case of identical director configuration [7] inside droplets and uniform distribution of LC droplet bipolar axes over the angle, we can write the average components of the vector amplitude scattering function and their squared absolute values (see Eqs. (1) and (2)) as follows:

$$\begin{aligned} \left\langle f_{vv}(\theta_s, \varphi_s) \right\rangle = {} & \left\langle S_2(\theta_s, \varphi_s) \right\rangle \overline{\cos^2(\varphi_s - \varphi_d)} + \left\langle S_1(\theta_s, \varphi_s) \right\rangle \overline{\sin^2(\varphi_s - \varphi_d)} + \\ & \frac{1}{2} \left\langle \left(S_3(\theta_s, \varphi_s) + S_4(\theta_s, \varphi_s)\right) \right\rangle \overline{\sin 2(\varphi_s - \varphi_d)} \end{aligned}, \tag{17}$$

$$\begin{aligned} \left\langle f_{vh}(\theta_s, \varphi_s) \right\rangle = {} & \left\langle S_3(\theta_s, \varphi_s) \right\rangle \overline{\sin^2(\varphi_s - \varphi_d)} - \left\langle S_4(\theta_s, \varphi_s) \right\rangle \overline{\cos^2(\varphi_s - \varphi_d)} + \\ & \frac{1}{2} \left\langle \left(S_2(\theta_s, \varphi_s) - S_1(\theta_s, \varphi_s)\right) \right\rangle \overline{\sin 2(\varphi_s - \varphi_d)} \end{aligned}, \tag{18}$$

$$\begin{aligned}
\left\langle |f_{vv}|^2 \right\rangle &= \left\langle |S_2|^2 \right\rangle \overline{\cos^4(\varphi_s - \varphi_d)} + \left\langle |S_1|^2 \right\rangle \overline{\sin^4(\varphi_s - \varphi_d)} + \\
&+ \frac{1}{4}\left\langle \left\{ S_1 S_2^* + S_2 S_1^* + (S_3 + S_4)(S_3^* + S_4^*) \right\} \right\rangle \overline{\sin^2 2(\varphi_s - \varphi_d)} + \\
&+ \frac{1}{8}\left\langle \left\{ (S_3 + S_4) S_2^* + S_2 (S_3^* + S_4^*) \right\} \right\rangle \left[2\overline{\sin 2(\varphi_s - \varphi_d)} + \overline{\sin 4(\varphi_s - \varphi_d)} \right] + \\
&+ \frac{1}{8}\left\langle \left\{ (S_3 + S_4) S_1^* + S_1 (S_3^* + S_4^*) \right\} \right\rangle \left[2\overline{\sin 2(\varphi_s - \varphi_d)} - \overline{\sin 4(\varphi_s - \varphi_d)} \right]
\end{aligned}, \tag{19}$$

$$\begin{aligned}
\left\langle |f_{vh}|^2 \right\rangle &= \left\langle |S_3|^2 \right\rangle \overline{\sin^4(\varphi_s - \varphi_d)} + \left\langle |S_4|^2 \right\rangle \overline{\cos^4(\varphi_s - \varphi_d)} + \\
&+ \frac{1}{4}\left\langle \left\{ (S_2 - S_1)(S_2^* - S_1^*) - S_4 S_3^* - S_3 S_4^* \right\} \right\rangle \overline{\sin^2 2(\varphi_s - \varphi_d)} - \\
&- \frac{1}{8}\left\langle \left\{ (S_2 - S_1) S_4^* + S_4 (S_2^* - S_1^*) \right\} \right\rangle \left[2\overline{\sin 2(\varphi_s - \varphi_d)} + \overline{\sin 4(\varphi_s - \varphi_d)} \right] + \\
&+ \frac{1}{8}\left\langle \left\{ (S_2 - S_1) S_3^* + S_3 (S_2^* - S_1^*) \right\} \right\rangle \left[2\overline{\sin 2(\varphi_s - \varphi_d)} - \overline{\sin 4(\varphi_s - \varphi_d)} \right]
\end{aligned}. \tag{20}$$

Here the overline designates averaging over azimuthal angle φ_d, the angle brackets $\langle \cdots \rangle$ in the right sides designates averaging over sizes of LC droplets.

In Eqs. (17)-(20):

$$\overline{\cos^2(\varphi_s - \varphi_d)} = \frac{1}{2}\left(1 + \cos 2\varphi_s \sin c 2\varphi_m\right), \tag{21}$$

$$\overline{\sin^2(\varphi_s - \varphi_d)} = \frac{1}{2}\left(1 - \cos 2\varphi_s \sin c 2\varphi_m\right), \tag{22}$$

$$\overline{\sin 2(\varphi_s - \varphi_d)} = \sin 2\varphi_s \sin c 2\varphi_m, \tag{23}$$

$$\overline{\cos^4(\varphi_s - \varphi_d)} = \frac{3}{8} + \frac{1}{2}\cos 2\varphi_s \,\mathrm{sinc} 2\varphi_m + \frac{1}{8}\cos 4\varphi_s \,\mathrm{sinc} 4\varphi_m, \tag{24}$$

$$\overline{\sin^4(\varphi_s - \varphi_d)} = \frac{3}{8} - \frac{1}{2}\cos 2\varphi_s \,\mathrm{sinc} 2\varphi_m + \frac{1}{8}\cos 4\varphi_s \,\mathrm{sinc} 4\varphi_m, \tag{25}$$

$$\overline{\sin^2 2(\varphi_s - \varphi_d)} = \frac{1}{2}\left(1 - \cos 4\varphi_s \sin c 4\varphi_m\right), \tag{26}$$

$$\overline{\sin 4(\varphi_s - \varphi_d)} = \sin 4\varphi_s \sin c 4\varphi_m, \tag{27}$$

where φ_m is the maximum azimuthal angle of droplet bipolar axes deviation from the *y* axis of laboratory frame. When $\varphi_m = 0$ and $\varphi_m = \pi$ the droplet bipolar axes are oriented along the *y* axis and randomly, respectively. When $0<\varphi_m<\pi$ the droplet bipolar axes are partially oriented. Eqs. (21)-(27) characterizes the orientation structure of PDLC monolayer. They can be called the orientation factors.

It is worth paying attention that the above equations are written for the case when vector $\mathbf{E}_i$ (Fig.6) is directed along the *y* axis. If they are unparalleled, the azimuthal scattering angle φ_s in the Eqs. (21)-(27) should be replaced by the α-φ_s, where α is the polarization angle.

The theoretical data are shown in Fig. 5 in comparison with experiment. The calculations are fulfilled with using the experimental histogram of LC droplet lateral size distribution in monolayer plane (Fig. 3). Internal orientation structure of LC droplets was determined using the solution of the problem of free energy volume density minimization [2,3,11].

6. Conclusion

For research of specific features of light scattering by PDLC film, the sample was prepared applying SIPS process of LC encapsulation. As a result, a monolayer of bipolar nematic droplets of oblate spheroidal shape was made with the in-plane diameters and anisometry ratio varying in the ranges of 6 - 20 μm and 0.7 - 0.2, respectively. It should be noted that the average anisometry ratio value 0.31 in our case is considerably less than the one for more thick PDLC film with multilayer arrangement of nematic droplets [10,11].

The developed light scattering calculation method based on the anomalous diffraction and interference approximations is a valid tool for describing real PDLC monolayer structures and can be used effectively for forecasting of properties of promising optical materials based on the LC dispersions.

Acknowledgments

The work was supported by the National Academy of Sciences of Belarus and the Russian Academy of Sciences in the framework of the InterAcademy (NASB–SB RAS) Integration Project; the Belarusian Republican Foundation for Fundamental Research (project F15SB-039), and the Russian Foundation for Basic Research (project No 15-02-06924).

References

[1] Stein RS, Rhodes MB. Photographic light scattering by polyethylene films. J Appl Phys 1960;31:1873-84.

[2] Zumer S, Doane JW. Light scattering from a small nematic droplet. Phys Rev A 1986;34:3373-86.

[3] Ondris-Crawford R, Boyko EP, Wagner BG, Erdmann JH, Zumer S, Doane JW. Microscope textures of nematic droplets in polymer dispersed liquid crystal. J Appl Phys 1991;69:6380–6.

[4] Ding J, Yang Y. Small angle light scattering from axial nematic droplets. Mol Cryst Liq Cryst 1994;238:47-60.

[5] Ding J, Yang Y. Small angle light scattering from bipolar nematic droplets. Mol Cryst Liq Cryst 1994;257:63-87.

[6] Leclercq L, Maschke U, Ewen B, Coqueret X, Mechernene L, Benmouna M. Light scattering from acrylate-based polymer dispersed liquid crystals: theoretical considerations and experimental examples. Liq Cryst 1999;26(3):415-25.

[7] Loiko VA, Zyryanov VYa, Maschke U, Konkolovich AV, Miskevich AA. Small-angle light scattering and transmittance of polymer film, containing liquid crystal droplets with inhomogeneous boundary conditions. JQSRT 2012;113:2585-92.

[8] Zyryanov VYa, Epshtein VS. Measurement of refractive-indexes of liquid-crystals using a tunable source of coherent infrared radiation. Instruments and experimental techniques. 1987;30(2):431-3.

[9] Zyryanov VY, Smorgon SL, Shabanov VF. Elongated films of polymer-dispersed liquid crystals as scattering polarizers. Molecular Engineering 1992;1:305-10.

[10] Drzaic PS. Reorientation dynamics of polymer dispersed nematic liquid-crystal films. Liq Cryst 1988;3(11):1543-59.

[11] Prishchepa OO, Shabanov AV, Zyryanov VYa, Parshin AM, Nazarov VG. Friedericksz threshold field in bipolar nematic droplets with strong surface anchoring. JETP Lett 2006;84(11):607-12.

[12] Loiko VA, Maschke U, Zyryanov VYa, Konkolovich AV, Miskevich AA. Angular structure of radiation scattered by monolayer of polydisperse droplets of nematic liquid crystal. Optics and spectroscopy 2011;110(1):866-72.

[13] Loiko VA, Maschke U, Zyryanov VYa, Konkolovich AV., Misckevich AA. Small-Angle Light Scattering from Polymer-Dispersed Liquid-Crystal Films. Journal of Experimental and Theoretical Physics 2008;107:692-8.

[14] Ziman JM. Models of Disorder. Cambridge: Univ. Press; 1979.

[15] Lock JA, Chiu CL. Correlated light scattering by a dence distribution of condensed droplets on a window pane. Appl Opt 1994;33(21):4663-71.

[16] Bohren CF, Huffman DR. Absorption and Scattering of Light by Small Particles. New York: Wiley; 1983.

[17] Hulst HC. Light scattering by small particles. New York: Dover publishing incorporations; 1957.

[18] Loiko VA, Konkolovich AV. Interference effect of coherent transmittance quenching: theoretical study of optical modulation by surface ferroelectric liquid crystal droplets. J Phys D Appl Phys 2000;33:2201-11.

[19] Zumer S. Light scattering from nematic droplets: Anomalous-diffraction approach. Phys Rev A 1988;37:4006-15.

[20] Meeten GH. Small-angle scattering by spherulites in the anomalous diffraction approximation. Opt Acta 1982;29:757–70.

[21] Loiko VA, Maschke U, Zyryanov VYa, Konkolovich AV, Miskevich AA. Coherent transmission and angular structure of light scattering by monolayer films of polymer dispersed liquid crystals with inhomogeneous boundary conditions. Optics and spectroscopy 2011;111(6):866-72.

[22] Simoni F. Nonlinear Properties of Liquid Crystals and Polymer Dispersed Liquid Crystals. Singapore: World Sci; 1997.

[23] Loiko VA, Miskevich AA, Konkolovich AV. Order parameter of elongated liquid crystal droplets: the method of retrieval by the coherent transmittance data. Phys Rev E 2006;74:031704-1-7.

[24] Loiko VA, Konkolovich AV, Miskevich AA. Reconstraction of the order parameter of oriented liquid crystal droplets. Opt and Spectr 2006;101:642-8.

[25] Krakhalev MN, Loiko VA, Zyryanov VYa. Electro-optical characteristics of polymer-dispersed liquid crystal film controlled by ionic-surfactant method. Technical Physics Letters 2011;37(1):34-6.